Food and Chemical Toxicology 126 (2019) 41–55

Contents lists available at ScienceDirect

Food and Chemical Toxicology

journal homepage: www.elsevier.com/locate/foodchemtox

Mangiferin alleviates arsenic induced oxidative lung injury via upregulation of the Nrf2-HO1 axis

Sushweta Mahalanobish[1], Sukanya Saha[1], Sayanta Dutta, Parames C. Sil*

Division of Molecular Medicine, Bose Institute, P-1/12, CIT Scheme VII M, Kolkata, 700054, India

ARTICLE INFO

Keywords:
Arsenic
Oxidative stress
Lung
Apoptosis
Inflammation
Mangiferin

ABSTRACT

Arsenic contaminated drinking water consumption is a serious health issue around the world. Chronic inorganic arsenic exposure has been associated with respiratory dysfunctions. It exerts various detrimental effects, disrupting normal cellular homeostasis and turning on severe pulmonary complications. This study elucidated the role of mangiferin, a natural xanthone, against arsenic induced lung toxicity. Chronic exposure of sodium arsenite ($NaAsO_2$) at 10 mg/kg bw for 3 months abruptly increased the LDH release in broncho-alveolar lavage fluid, generated reactive oxygen species (ROS), impaired the antioxidant defense and distorted the alveoli architecture. It caused significant inflammatory outburst and promoted the apoptotic mode of cell death via upregulating the expressions of various proapoptotic molecules related to mitochondrial, extra-mitochondrial and ER stress mediated apoptotic pathway. Activation of inflammatory cascade led to disruption of alveolar capillary barrier and impaired Na^+/K^+-ATPase function that led to detaining of alveolar fluid clearance activity. Mangiferin due to its anti-inflammatory activity suppressed this inflammation and reduced inflammatory cell infiltration in lung tissue. It significantly restored the antioxidant balance and inhibited apoptosis in lung via upregulating Nrf2-HO1 axis.

1. Introduction

The environmental and occupational hazards of the contemporary world make us greatly predisposed to different forms of heavy metals toxicity. Most prevailing sources of these metals exposure include groundwater contamination, tanning, mining etc. (Leonard et al., 2004). In this field of metal intoxication, arsenic (As) is one of the most widely studied elements. It is a metalloid found mainly in water, air, soil, and exists in organic as well as inorganic forms (Tseng, 2009). Inorganic forms of As include trivalent meta-arsenite (As^{3+}) which is present mainly in deep anoxic wells whereas its pentavalent arsenate form (As^{5+}) exists mostly in surface water. Moreover, International Agency for Research on Cancer (IARC) has declared inorganic As as a potent carcinogen. Usually, ingestion and inhalation is the main route of As entry in the human body. As exposure takes place primarily via contaminated drinking water in the mainly affected countries like India, Bangladesh, China, Central America and South America. Detection of As in contaminated food or drinking water is very tough due to its colorless and odorless nature and thus it silently promotes serious health hazards. It has been reported that the concentration of As in drinking water in Argentina (200 ppb) Mexico (400 ppb) (García-Vargas et al., 1991), Taiwan (50–1980 ppb) (Yen et al., 2007), and the Indo-Bangladesh region (800 ppb) is well above the WHO guidelines of the maximum permissible value (10 ppb) (Chakraborti et al., 2010, Chowdhury et al., 2000). It is noteworthy that inorganic As ingestion is not only associated with cancer progression (Bulka et al., 2016; Lynch et al., 2017; Mazumder et al., 1998) but it also makes individuals susceptible to develop multiple organ diseases including cardiovascular (States et al., 2009), reproductive (Kim and Kim, 2015), and neurotoxic (Das et al., 2009; Saha et al., 2018; Tyler and Allan., 2014) effects among adults and children population.

In recent years, lung has gained increasing attention as it is a uniquely susceptible target organ for orally ingested As. Several epidemiological studies reported the association between chronic As exposure and nonmalignant respiratory effects such as impaired lung function (Das et al., 2014; Dauphine et al., 2011; Parvez et al., 2008; Recio-Vega et al., 2015; von Ehrenstein et al., 2005; Wei et al., 2018), chronic obstructive pulmonary disease, pneumonia, bronchiectasis and so on. Although intricate signaling mechanism in the context of chronic As exposure induced increased chances of lung injury are poorly understood, several research in rodent models showed that some methylated form of As species are favorably distributed to the lung tissue

* Corresponding author. Division of Molecular Medicine, Bose Institute, P-1/12, CIT Scheme VII M, Calcutta, 700054, West Bengal, India.
E-mail addresses: parames_95@yahoo.co.in, parames@jcbose.ac.in (P.C. Sil).
[1] Authors have contributed equally.

https://doi.org/10.1016/j.fct.2019.02.022
Received 14 November 2018; Received in revised form 15 January 2019; Accepted 8 February 2019
Available online 12 February 2019
0278-6915/

owing to presence of arsenite methyltransferase that efficiently metabolizes As in lung (Healy et al., 1998; Hughes et al., 2003; Kenyon et al., 2005). It has been found that As directly induces the production of reactive oxygen species (ROS) leading to lipid peroxidation (LPO), causing oxidative damage (Manna et al., 2007; Rashid et al., 2013; Sinha et al., 2007, 2008). People drinking As polluted water for a long time, increased MDA levels in the lung along with a decrease in glutathione (GSH) and catalase (CAT) activity, causing a striking imbalance of antioxidants pro-oxidants ratio and also induced DNA strand break, ultimately causing impaired lung functions (Yamanaka et al., 1989). Oral As ingestion significantly altered DNA methylation, causing expression in the modification of pulmonary genes (Andrew et al., 2007; Boellmann et al., 2010).

In recent years, natural bioactive compounds has gained more attention as protective molecules in the field of pathophysiology (Das et al., 2012a,b; Ghosh and Sil., 2013; Rashid and Sil., 2015; Sarkar et al., 2006). Polyphenols are the major group of natural bioactive antioxidants due to their ability of inducing antioxidant enzymes gene expression as well as possessing various antioxidant properties like free radical scavenging, hydrogen donating, and so on (Bhattacharya et al., 2017; Das et al., 2012a,b; Pal et al., 2013, 2014; Saha et al., 2016). Especially, mangiferin (2-C-β-D-glucopyranosyl-1, 3, 6, 7-tetrahydroxyxanthone), a xanthonoid obtained from Anacardiaceae and Gentianaceae families, is used as a unique source of potential therapeutic agent (Yoshimi et al., 2001). Due to its iron chelating ability via Fenton-type reactions, mangiferin potentially suppressed the free radicals production. Different studies revealed that mangiferin showed antioxidant (Moreira et al., 2001), antitumor (Guha et al., 1996), antidiabetic (Das et al., 2012a,b) and immunomodulatory activities (Rodeiro et al., 2014). Having xanthone backbone, it has the ability to scavenge ROS, inhibit LPO, and increase the reduced glutathione content. Moreover, it can alter the expression of apoptosis-related genes, thus playing a very crucial role in apoptosis regulation. So far, there is no study describing the protective role of mangiferin against As induced oxidative damage in lung. In this present study, we investigate whether this polyphenol was effective in combating the oxidative damage by As in lung and its mechanism of protective action. We also showed that the generation of oxygen radicals by As was successfully neutralized by mangiferin. It protected the lung via Nrf2-HO1 signaling pathway from oxidative stress mediated lung injury.

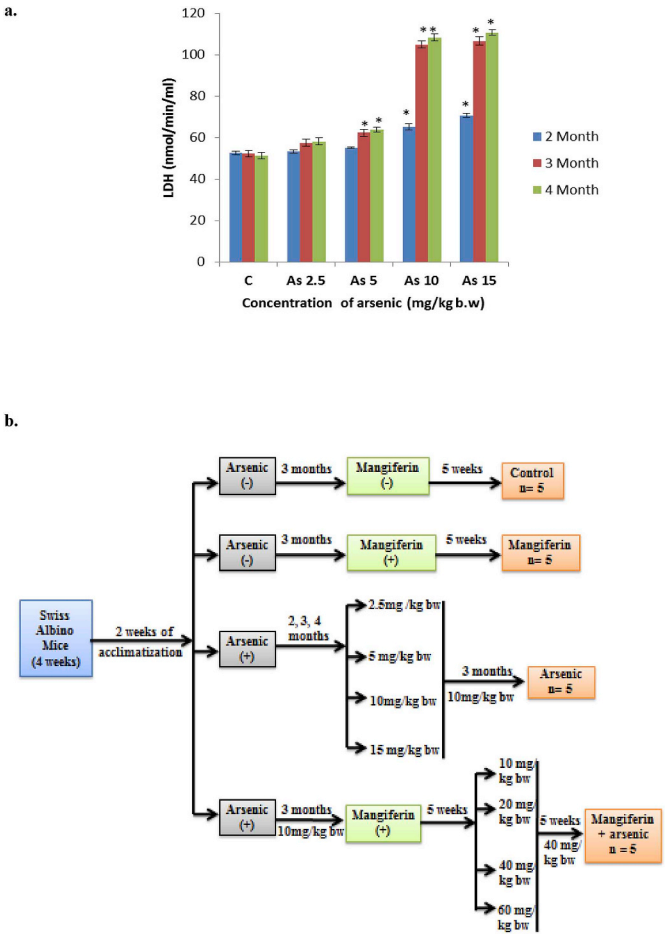

Fig. 1. (a) Dose dependent assay to determine arsenic toxicity in experimental mice model by analyzing LDH leakage assay in BALF. C: normal control mice; As: arsenic intoxicated mice. Each data represents the mean ± SD of 5 independent experiments for each individual group. *Significant difference between the control and arsenic exposed toxic group ($*P < 0.05$). **(b)** Schematic diagram of the animal experimental protocol.

2. Materials and methods

2.1. Chemicals

Mangiferin, Sodium arsenite ($NaAsO_2$), LDH assay kit and Apoptosis detection kit was purchased from Sigma-Aldrich Chemical Company (St. Louis, MO, USA). The primers used for RT-PCR were purchased from Integrated DNA Technologies (IDT) and GCC Biotech. The antibodies were purchased from Abcam (Cambridge, UK), Sigma-Aldrich Chemical Company (St. Louis, USA), Cell Signaling Technology (Danvers, MA 01923) and Biobharati life sciences (West Bengal, India) Other necessary chemicals and reagents were of analytical grade and purchased from the SISCO Research Laboratory, Mumbai, India.

2.2. In vivo model for As induced chronic pulmonary injury

Male Swiss albino mice, 4 weeks old were obtained from Central Animal house and research facility of Bose Institute Kolkata, India. All the animals were accustomed for 2 weeks in an alternating 12 h light/dark cycles and provided with water ad libitum and standard dietary food. These 6 weeks old acclimatized mice weighing 20–25 g were used for this experimental purpose. All the studies in animals were performed following the guidelines of the Institutional Animal Ethical Committee (IAEC), Bose Institute, Kolkata (with the permit number IAEC/BI/3(I) cert./2010) and full details of the work plan with experimental animals were approved by IAEC as well as CPCSEA (Committee for the Purpose of Control and Supervision on Experiments on Animals), Ministry of Environment and Forests, New Delhi, India (the permit number is: 1796/PO/Ere/S/14/CPCSEA). To develop *in vivo* models of As induced pulmonary injury, a pilot study was done to determine the optimum dose and time dependent effects of $NaAsO_2$. It was given orally (in drinking water) at a dose of 2.5, 5, 10, 15 mg/kg bw for each 2, 3 and 4 months. After analyzing the lactate dehydrogenase (LDH) level in broncho alveolar lavage fluid (BALF), no significant difference of toxicity was found in 10 mg/kg bw and 15 mg/kg bw in 3 and 4 months respectively. Thus 10 mg/kg bw for 3 months had been chosen as the optimum dose of As toxicity (Fig. 1a). Similar pilot study was done to determine the optimum dose and time dependent effects of mangiferin. It was given via oral gavage at a dose of 10, 20, 40, 60 mg/kg bw for each 4, 5, 6 weeks. When we analyzed the LDH level in BALF

of this As-intoxicated mangiferin treated group, no significant difference in protection was found in between the groups 40 mg/kg bw and 60 mg/kg bw in 5 and 6 weeks respectively. So the optimum dose of mangiferin's protection against As intoxication was chosen as 40 mg/kg bw for 5 weeks.

Animals were divided into four groups consisting of five animals in each group.

Group 1: Swiss albino mice receiving vehicle served as control group.
Group 2: Swiss albino mice received mangiferin (40 mg/kg bw) for 5 weeks served as mangiferin treated group.
Group 3: Swiss albino mice received $NaAsO_2$ administration (10 mg/kg bw) for 3 months and served as As group.
Group 4: Swiss albino mice received mangiferin (40 mg/kg bw for 5 weeks) after $NaAsO_2$ administration (10 mg/kg bw for 3 months).

Fig. 1b shows a schematic diagram of the animal experimental protocol.

2.3. Collection of BALF and differential cells count

At the end of the experimental procedure, the mice were fasted for 12 h, then weighed and subjected to sacrifice and tracheotomy was performed. BALF was collected by lavage with ice-cold phosphate buffered saline (PBS, 500 µl × 3; 75–80% of the lavage volume was recovered) via the tracheal catheter. Then BALF was centrifuged (3000 rpm for 10 min at 4 °C) and the supernatants were kept at −80 °C to analysis markers of pulmonary toxicity. The pellet was resuspended in ice-cold PBS, centrifuged in cytospin and stained with Wright–Giemsa staining for 5 min and subjected for differential cells count by light microscopy on the basis of their morphology. Total number of cells present in BALF was subjected to quantify by using hemocytometer.

2.4. LDH assay, total protein measurement and TNF-α level in BALF

Lavage supernatant was used for LDH assay where the reduction of nicotinamide adenine dinucleotide was monitored spectrophotometrically (450 nm) in the presence of lactate. LDH assay was performed according to manufacturer's protocol. Total protein content in the BALF was assessed by using BCA assay method. TNF-α level in BALF was measured by commercially available ELISA kit (Span Diagnostic, India).

2.5. Measurement of lung wet/dry weight ratio

After completion of BALF collection, both lobes of the lung was aseptically removed, rinsed with ice cold-PBS, and weighed. After wet weight (W) was measured, 100 mg of lung tissue was kept for drying at 60 °C for 48 h to reach a constant weight, which is called the dry weight (D). The ratio of W/D weight was calculated.

2.6. As content in lung tissue

In the lung tissue of experimental animal groups, the As content was determined according to the method of DAS et al. (Das et al., 1996) using Atomic Absorption Spectrophotometer (Perkin Elmer Model No. 3100).

2.7. Lung histopathology

Lung from different experimental mice group were fixed in 10% neutral buffered formalin and embedded in paraffin. After paraffin embedding, 5 µm thick sections were cut and stained with hematoxylin and eosin (H&E) and observed under light microscope (at 40× magnification) to assess histological alteration.

2.8. Myeloperoxidase (MPO) assay

The level of MPO was assessed to determine neutrophil accumulation into the lung. Briefly, 10 µl of freshly prepared lung tissue homogenate was mixed with freshly prepared 110 µl of 3,3′-5,5′-tetramethylbenzidine (TMB) reagent and 80 µl of H_2O_2 (0.75mmM) and incubated at 37 °C for 5 min. The reaction was stopped after the addition of 50 µl of 2 M H_2SO_4 and activity was measured spectrophotometrically at 450 nm and expressed as µmol of H_2O_2 consumed per min/mg protein.

2.9. Determination of intracellular ROS production

The intracellular ROS were measured from lung tissue homogenate following the method of Saha et al. (2018). Briefly, 100 µg of protein from lung tissue lysate was incubated at 37 °C for 15 min in assay media containing 20 mM Tris–HCl, 130 mM KCl, 5 Mm $MgCl_2$, 20 mM NaH_2PO_4, 30 mM glucose, 5 µM DCF-DA. Formation of the fluorescent DCF (oxidized form of DCF-DA) was monitored with 488 nm (excitation wavelength) and 510 nm (emission wavelength) wavelengths respectively.

2.10. LPO and protein carbonylation assay

The extent of LPO in the lung was determined via reactive interaction between lipid and thiobarbituric acid (TBA) as described by Esterbauer and CheeSDan (Hughes et al., 2011). The evaluation was based on the formation of thiobarbituric acid reactive substance (TBARS) at 532 nm and finally the concentration was calculated.

To determine the protein carbonyl content, method of Uchida and Stadtman was followed (Uchida and Stadtman, 1992). Samples were mixed with equal amounts of 0.1% (w/v) 2, 4-DNPH (in 2 N HCl) and incubated at room temperature for 1 h. 20% TCA was added in this solution and then the precipitate was collected following centrifugation. This precipitate was dissolved into guanidine hydrochloride in 133 mM tris solution having 13 mM EDTA. Next at 365 nm, the absorbance was measured and concentration was calculated as nmol/mg protein.

2.11. Estimation of intracellular antioxidant enzymes and metabolites

The various intracellular antioxidant enzymes in lung tissue were assessed by estimating activities of superoxide dismutase (SOD), catalase (CAT), Glutathione S-Transferase (GST), Glutathione Reductase (GR) and Glutathione Peroxidase (GPx) (Dutta et al., 2018). The levels of reduced (GSH) and oxidized glutathione (GSSG) were measured according to the protocol of Hissin and Hilf (1976)

2.12. DNA fragmentation assay

Genomic DNA was isolated from lung tissue following the method of Huang et al. (2007). After isolation, the genomic DNA was subjected to agarose gel electrophoresis. DNA fragmentation was analyzed through DNA ladder formation in the presence of UV light.

2.13. Determination of mitochondrial membrane potential (MMP)

Lung was isolated, washed in ice-cold PBS, and homogenized in mitochondrial isolation buffer (MIB) and centrifuged at 750 × *g*, 4 °C for 10 min. This supernatant (1) was kept in ice. The resulting pellets was resuspended in 500 µl of MIB, homogenized and again centrifuged at 750 × *g*, 4 °C for 10 min. Now this supernatant (2) was mixed with supernatant (1) and re-centrifuged at 10,000 × *g*, 4 °C for 5 min. Then the pellet was resuspended in 400 µl of MIB. Now, it was subjected for MMP assay by using JC1 dye (cationic fluorescent dye) (Lampl et al., 2015; Perelman et al., 2012).

2.14. Evans blue assay to determine capillary barrier disruption

Pulmonary capillary permeability in lung was detected by measuring Evans blue dye concentrations. 5% sterile solution of Evans blue was prepared and 200 µl of Evans blue solution was gently injected in mouse through the lateral tail vein. After 30 min of injection, cardiac perfusion was performed under deep anesthesia and lung was collected. Then lung was homogenized in 1 ml of PBS, extracted in 2 ml of formamide (24 h, 60 °C) and centrifuged (5000 × *g*, 30 min, and 20 °C). The supernatants were collected and absorbance was measured spectrophotometrically at 620 nm.

2.15. Na^+/K^+-ATPase activity

Na^+/K^+-ATPase assay was performed following the protocol of Harris et al. (1996). Na^+/K^+-ATPase activity was determined in 100 µL freshly prepared baso-lateral fractionation of lung homogenate in the presence and absence of 2 mM ouabain. Ouabain-sensitive Na^+/K^+-ATPase activity was measured by determining the ouabain-inhibitable portion of the ATPase activity. Liberated inorganic phosphate was measured spectrophotometrically at 820 nm.

2.16. RNA extraction and reverse transcriptase PCR (RT-PCR)

RNA was extracted from lung samples of mice using the TRIzol reagent according to the Manufacturer's protocol (Invitrogen). Amount of RNA was measured using nanodrop. Then 2 µg of extracted RNA/sample was converted to cDNA using Thermo Scientific Verso cDNA synthesis kit (Thermo Scientific, USA). Thermal cycling was performed in thermal cycler (2720 Thermal Cycler, Thermo Fisher Scientific). The cDNA samples were initially denatured at 95 °C for 5 min followed by the successive steps (in each cycle): 30 s at 95 °C for denaturation, 30 s for primer annealing at specific annealing temperature, and 45 s at 72 °C for primer extension. This was continued upto 35 cycles and then DNA extension was performed for 5 min at 72 °C. The amplification products were held at 4 °C and finally subjected to agarose gel electrophoresis. The exact product size and annealing temperatures of the primers used are shown in Table 1.

2.17. Immunoblot analysis

To perform immunoblot analysis, equal amounts of protein samples (40µg/lane) from individual lung tissue homogenate were loaded and separated by sodium dodecyl sulfate –polyacrylamide gel electrophoresis (SDS–PAGE). Then protein was transferred on PVDF membrane and the membrane was subjected to blocking (using 5% BSA for 2 h at room temperature) to prevent non-specific antibody binding. Membrane was then subjected to incubation with primary antibodies at 4 °C for overnight. Next day, membranes were carefully washed in TBST for 30 min and incubated with HRP-conjugated secondary antibody for 2 h at room temperature following which washed in TBST again. Afterward, the membranes were developed by ECL solution using HRP as substrate.

2.18. Immunofluorescence

Lung tissues were fixed in 10% buffered formaldehyde solution and embedded in paraffin. 5 µm thick tissue sections were deparaffinised in xylene and rehydrated (with ethanol: water down gradation). The slides were immersed in antigen retrieval buffer for 15 min at room temperature and then subjected to blocking for 2 h. The slides were incubated overnight at 4 °C with the anti-TNF-α antibody (dilution 1:100). We used goat anti-rabbit H&L (FITC)-linked secondary antibody to co-localize the primary antibody and mounted the slide with DPX. Finally the slides were observed under Leica Microsystem DN1000 (camera: DFC450 C) microscope (Saha et al., 2018).

2.19. Statistics

Results were expressed as mean ± SD (where n = 5). Statistical evaluation was performed using the Origin8 software (OriginLab, Massachusetts) by means of one way analysis of variance (ANOVA) and the group means were compared by Tukey test. The *P*-value ≤ 0.05 was considered as statistically significant.

3. Results

3.1. Mangiferin ameliorated As induced cytotoxicity and airway inflammation in the lung tissue

BALF LDH activity is an important marker of cell toxicity. Level of LDH in BALF of As intoxicated mice was elevated in a significant level compared to control group (Fig. 2a). Furthermore, in As intoxicated group a high level of total protein concentration in BALF, indicating alveolar-capillary permeability and/or alveolitis, was found (Fig. 2b).

Table 1
Shows the product size and annealing temperatures of the primers used in this study.

GENE	PRIMER SEQUENCE (5′ TO 3′)	ANNEALING TEMPERATURE(°C)	APLICON SIZE (bp)
β-actin	FP: GAATGGCCCAGGTCTGAGGC RP: GTCAGTGTACAGGCCAGCCC	60.2	120
TNF-α	FP: TCTCAGAATGAGGCTGGATAAG RP: CCCGGCCTTCCAAATAAATAC	55	188
IL-1β	FP: GAGTGTGGATCCCAAGCAATA RP: TCCTGACCACTGTTGTTTCC	45	174
IL-6	FP: GATAAGCTGGAGTCACAGAAGG RP: TTCTGACCACAGTGAGGAATG	58.7	163
MCP-1	FP: GAAGGAATGGGTCCAGACATAC RP: CACTCCTACAGAAGTGCTTGA	55	190
ICAM-1	FP:GTAGATCAGTGAGGAGGTGAATG RP: TGCCAGTCCACATAGTGTTTAT	58.7	170
VCAM-1	FP: CTAAGACTGAAGTTGGCTCAC RP: CACCAGACTGTACGATCCTTTC	58.7	188
VEGF	FP: GTCCCATGAAGTGATCAAG RP: GCTTGAAGATGTACTCTATC	56	116
Occludin	FP: CAGGAGGCTATAGCCATTG RP: GACTTATCATACCGATCCATC	59	107
ZO-1	FP: GATAGGAGTGCAAGCAGG RP: CAATCGAAGACCATATTCTTC	58	135

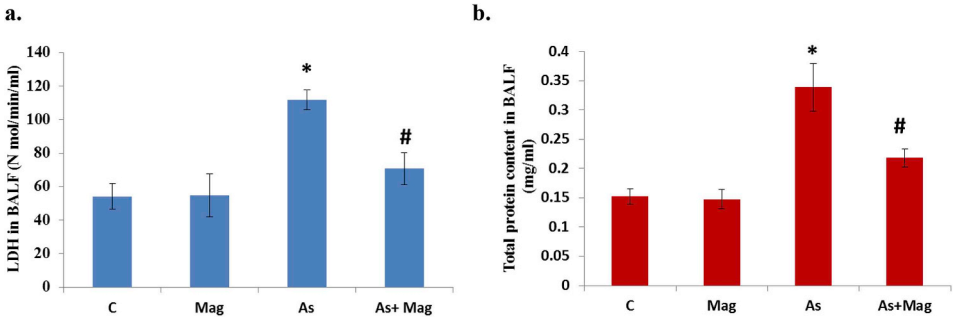

Fig. 2. Role of arsenic (As) and mangiferin (Mag) in **(a)** LDH level in BALF of Swiss albino mice. **(b)** Total protein concentration in the BALF. C: normal control mice; Mag: mangiferin administered mice; As: arsenic intoxicated mice; As + Mag: mangiferin post treatment after arsenic intoxication. Each data represents mean ± SD of 5 independent experiments for each individual group. *Significant difference between the control and arsenic exposed toxic group (*$P < 0.05$). #Significant difference between the arsenic exposed group and mangiferin post treated arsenic intoxicated group (#$P < 0.05$).

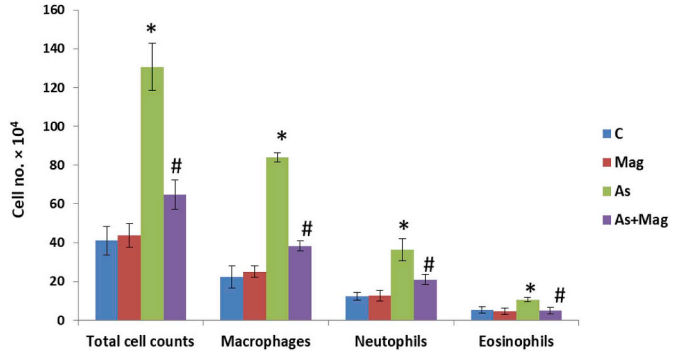

Fig. 3. Total cells and differential cells count in BALF of experimental animals. C: Normal control mice; Mag: mangiferin-administered mice; As: arsenic-intoxicated mice; As + Mag: mangiferin post treatment after arsenic intoxication. Each data represents mean ± SD of 5 independent experiments for each individual group. *Significant difference between the control and arsenic exposed toxic group (*$P < 0.05$). #Significant difference between the arsenic exposed group and mangiferin-post treated arsenic intoxicated group (#$P < 0.05$).

Mangiferin administration restored the LDH leakage level and total protein concentration in BALF.

Airway inflammation was determined by calculating the number of total and differential cells in BALF. Compared with the control group, there was a marked increase in the total numbers of cells as well as the percentage compositions of macrophages, neutrophils, and eosinophils in BALF of As intoxicated mice. Mangiferin post administration induced a significant decrease in the number of both total and individual cells counts (Fig. 3).

3.2. Alteration of lung W/D weight ratio and effect of mangiferin

Chronic As exposure caused a significant rise of W/D weight ratio of lung mass in experimental mice models. Mangiferin administration in As exposed mice caused reduction of lung W/D ratio (Fig. 4a).

3.3. Accumulation of As in lung was decreased after mangiferin administration

Huge accumulation of As was found in the lung tissue of As intoxicated group. Mangiferin significantly decreased the As content in lung tissue, showing its ability in the clearance of As from the lung tissue (Fig. 4b).

3.4. Mangiferin improved histopathological alteration and inhibited infiltration of inflammatory cells in As exposed lung tissue

In As exposed group, ruptured alveoli with increased alveolar thickness, inflammatory cell infiltration and hyperemia were noticed (Fig. 5a–b).

MPO, a biomarker of inflammatory cells infiltration, is associated with the onset of various pro-inflammatory and pro-oxidative responses. In the lung tissue of As exposed mice, MPO level was hugely up regulated (Fig. 6). Mangiferin administration considerably reduced the negative histological alterations and the level of MPO.

3.5. Mangiferin reduced oxidative insult and associated complications in As intoxicated lung tissue

The oxidative injury in lung due to chronic As exposure was estimated by measuring the level of ROS in lung tissue homogenate. The ROS level was abruptly upregulated in As intoxicated lung tissue (as reflected by the increasing intensity of DCF fluorescence compared to control group) (Fig. 7).

Free radicals are generated due to oxidative attack on lipids and protein that lead to the loss of their functions. Thus the level of MDA (marker of LPO) and protein carbonyl content (marker of protein damage) were measured in lung tissue homogenate. Significant level of LPO and protein carbonylation was observed in As intoxicated lung tissue compared to the respective control groups (Fig. 8a–b).

The levels of antioxidant enzymes SOD, CAT, GST, GR and GPX got significantly decreased in As intoxicated lung tissue. Again, GSH (thiol based antioxidant of the cell) level was also decreased significantly

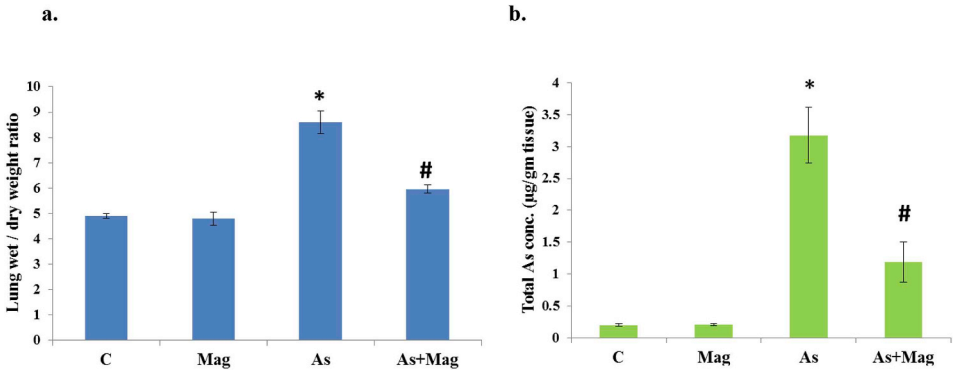

Fig. 4. Effect of arsenic (As) and mangiferin (Mag) in **(a)** Lung W/D weight ratio. **(b)** Arsenic accumulation in the lung tissue of the experimental mice. C: normal control mice; Mag: mangiferin administered mice; As: arsenic intoxicated mice; As + Mag: mangiferin post treatment after arsenic intoxication. Each data represents mean ± SD of 5 independent experiments for each individual group. *Significant difference between the control and arsenic exposed toxic group (*$P < 0.05$). #Significant difference between the arsenic exposed group and mangiferin post treated group (#$P < 0.05$).

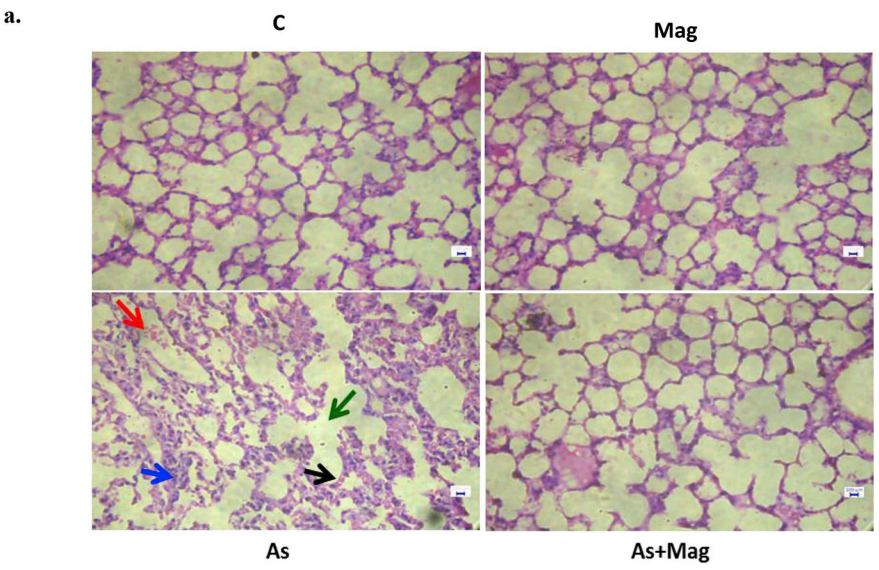

Fig. 5. Role of mangiferin on arsenic-induced lung injury in Swiss albino mice **(a)** Histological examination (H&E stained, 40x) in lung tissue was given in box. C group and mag group showed normal pulmonary architecture. As intoxicated group showed alveolar collapse with increased alveolar septum thickness, inflammatory cell infiltration, hyperemia in the lung tissue. Mangiferin treatment with optimum dose showed marked improvement of pulmonary architecture. **(b)** Representative micrographs of C, Mag, As and As + Mag mice group were shown along with total histological score, calculated based on alveolar collapse (green arrow), alveolar septum thickness (black arrow), inflammatory cells infiltration (blue arrow), and hyperemia (red arrow). Score indicating 0 as absent/none, 1 as mild, 2 showing moderate, and finally 3 for severe injury. C: normal control mice; Mag: mangiferin administered mice; As: arsenic intoxicated mice; As + Mag: mangiferin post treatment after arsenic intoxication. Each data represents the mean ± SD of 5 separate experiments in each individual group. *Significant difference between the control and arsenic exposed group (*$P < 0.05$). #Significant difference between arsenic exposed groups and mangiferin post treated arsenic intoxicated group (#$P < 0.05$). (For interpretation of the references to color in this figure legend, the reader is referred to the Web version of this article.)

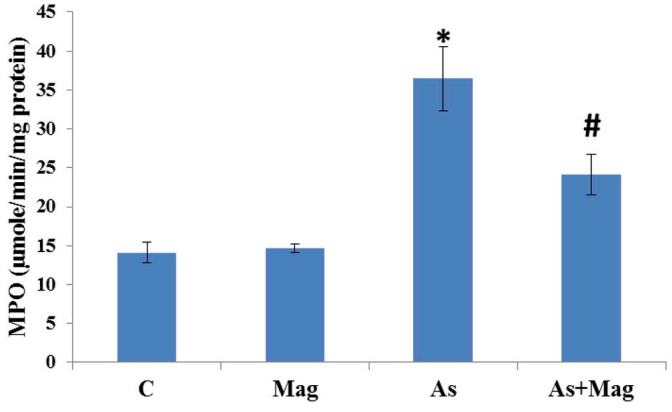

Fig. 6. Level of MPO activity different groups of lung tissue in experimental mice. C: normal control mice; Mag: mangiferin administered mice; As: arsenic intoxicated mice; As + Mag: mangiferin post treated arsenic intoxicated mice; Each data represents the mean ± SD of 5 independent experiments for each individual group. *Significant difference between the control and As exposed toxic group (*$P < 0.05$). #Significant difference between the arsenic exposed group and mangiferin post treated arsenic intoxicated group (#$P < 0.05$).

whereas it's oxidized form GSSG got increased on As administration in lung tissue (Fig. 9a-f).

Mangiferin administration successfully decreased the level of ROS, LPO and protein carbonylation in As induced lung tissue. It also caused substantial elevation of intracellular antioxidants in intoxicated lungs.

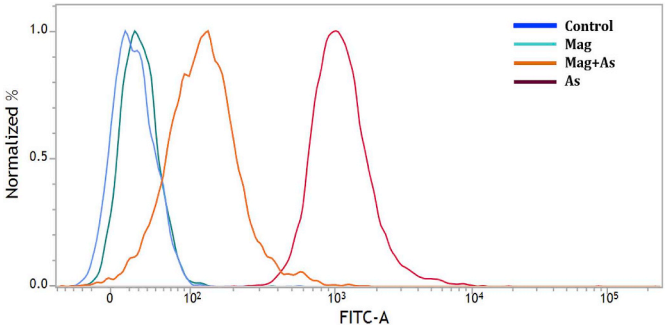

Fig. 7. Flow cytometric analysis of intracellular ROS production in the lung tissues of different experimental mice groups. H_2DCFDA staining showed increased production of ROS upon arsenic intoxication and its level was decreased upon mangiferin post administration in the experimental mice groups. Intracellular level of ROS was measured by the fluorescence intensity of DCF, the oxidized derivative of H_2DCFDA. C: normal control mice; Mag: mangiferin administered mice; As: arsenic intoxicated mice; As + Mag: mangiferin post treated arsenic intoxicated mice.

3.6. Mangiferin attenuated inflammatory cytokine outburst, decreased the level of junctional proteins and restored the alveolar-capillary barrier disruption in As intoxicated lung tissue

To investigate the role pro-inflammatory cytokines in As mediated pulmonary injury, we measured the level of TNF-α in BALF. Level of TNF-α got elevated in BALF of As intoxicated group (Fig. 10a). On

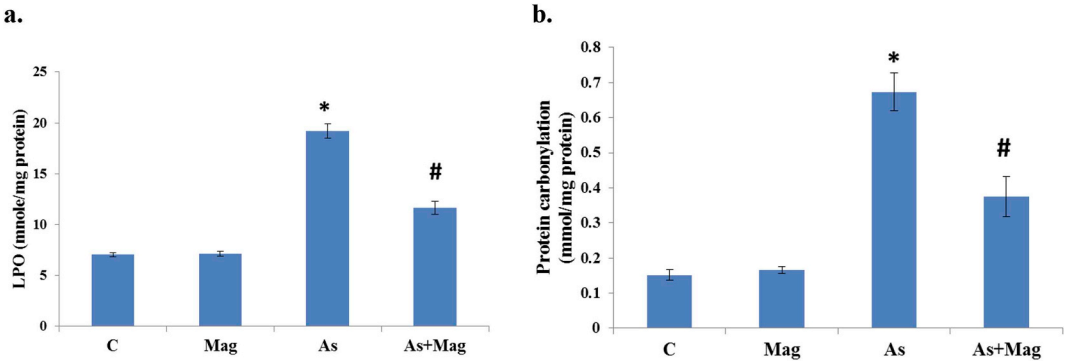

Fig. 8. Effect of arsenic and mangiferin on **(a)** LPO **(b)** protein carbonylation. C: normal control mice; Mag: mangiferin administered mice; As: arsenic intoxicated mice; As + Mag: mangiferin post treated arsenic intoxicated mice; Each data represents the mean ± SD of 5 independent experiments for each individual group. *Significant difference between the control and arsenic exposed toxic groups (*$P < 0.05$). #Significant difference between the arsenic exposed group and magiferin post treated arsenic intoxicated group (#$P < 0.05$).

measuring its mRNA level, we observed an increase in the As administered animals. This activated TNF-α in turn upregulated the production of Il-1β and IL-6. Further, upregulation of MCP-1, ICAM-1, VCAM-1, and VEGF as well as downregulation of junctional proteins (Occludin, ZO-1) led to increased inflammatory cell infiltration and endothelial vascular permeability in lung tissue of As intoxicated mice (Fig. 10b).

As intoxication caused significant disruption of the alveolar-capillary barrier as evidenced by increased uptake of Evan's blue dye in toxin administered lung tissue (Fig. 11).

Mangiferin administration decreased the level of pro-inflammatory cytokines and restored the alveolar-capillary barrier integrity by increasing the levels of junctional proteins.

3.7. Mangiferin provided protection against As induced functional impairment of Na^+/K^+ - ATPase and NF-κB upregulation

As intoxication inhibited the Na^+/K^+-ATPase function in lung tissue, resulting in repressed fluid clearance from lung. Mangiferin post administration successfully restored the Na^+/K^+-ATPase function to the normal level in lung (Fig. 12a). Moreover, the increased expression of NF-κB (regulatory molecule of Na^+/K^+ - ATPase) in the intoxicated lung was decreased upon mangiferin administration (Fig. 12b).

3.8. Mangiferin inhibited apoptotic cell death, alteration in Bax/Bcl2 ratio and ER stress in As induced lung

DNA fragmentation assay was done to confirm apoptotic mode cell death. The appearance of ladder pattern in DNA in the As intoxicated lung tissue assured that As intoxication led to apoptosis (Fig. 13).

Immunoblot analysis showed that there was an upregulation of Bax/Bcl2 ratio in As intoxicated mice. Upregulated Bax/Bcl2 ratio indicated the disrupted mitochondrial health (Fig. 14a). To assure this, MMP assay was performed using JC1 dye by FACS analysis. MMP was found to be significantly decreased due to As exposure (Fig. 14b).

Again, TNF-α upregulation and MMP disruption indicated that As induced apoptosis in lung tissue involved mitochondrial as well as extra-mitochondrial pathways. Therefore, on examining the apoptotic cascade we found that As exposure caused the upregulation of caspase 8 via the activation of TNF-α (Fig. 15a). Again, release of the cytochrome c from the mitochondria triggered caspase 9 activation. These caspases ultimately caused downstream caspase 3 activation (Fig. 15b). Moreover, there was increased fluorescence intensity of TNF-α in the tissue section of intoxicated lung (Fig. 15c).

Immunoblot analysis also revealed upregulated expression of PKC δ mediated JNK and subsequent activation of downstream CHOP and caspase 12 in As intoxicated group indicating ER stress (Fig. 15d).

Mangiferin administration substantially restored MMP, inhibited apoptosis and suppressed ER stress by downregulating the expression of apoptotic molecules, PKC δ and TNF-α.

3.9. Mangiferin showed antioxidant activity by upregulating Nrf2, HO1 and SOD2 expression

In mangiferin post treated As intoxicated group, Nrf2 got activated and was translocated to the nucleus to upregulate the expression of HO1 and SOD2. All these molecules showed decreased expression in As intoxicated animals (Fig. 16).

4. Discussion

A serious type of heavy metal toxicity is caused mainly due to consumption of As via drinking water (Henderson et al., 2017). High As exposure for a long time causes severe respiratory diseases by promoting oxidative stress. Mangiferin, a xanthonoid polyphenol, is known for its several medicinal properties (Ghosh et al., 2012; Saleh et al., 2014; Sinha et al., 2013). Here, we studied the detailed signaling mechanism of As mediated pulmonary toxicity and assessed the role of mangiferin as a protective antioxidant and anti-inflammatory molecule against chronic As induced lung injury. Primarily, to evaluate the amplitude and characteristics of inflammatory response we measured LDH level and total protein concentrations. Both the parameters were highly elevated indicating inflammatory pulmonary injury mediated cell damage. A significant increase in the total number of cells mainly macrophages and neutrophils were observed in BALF of As intoxicated mice showing progressive pulmonary toxicity. It has been found that increased lung W/D weight ratio manifests lung inflammation and injury (Hashizume et al., 2014; Matsuyama et al., 2008). In our experiment, increased W/D weight ratio in the lung of As intoxicated mice indicated inflammation and increased water permeability. Analyzing H&E stained histological tissue sections; we found there were significant structural alterations in the As intoxicated lung like wide areas of lung collapse, increased thickness alveolar septum, increased inflammatory cell infiltration and hyperemia in the alveoli. Mangiferin post treatment successfully prevented these upregulated toxic lung parameters and restored disrupted pulmonary architecture into normal level.

Generally, increased MPO expression is correlated with increased infiltration of neutrophils and macrophages. In As intoxicated lung tissue, MPO upregulation triggered pro-oxidant as well as inflammatory cascades. In our study, we also found that As elevated the intracellular ROS production. Then, to find out representative outcome of As mediated ROS production, we measured the level of LPO and protein carbonyl content in As intoxicated lung tissue. Additionally, we assessed the activity of various antioxidant enzymes like SOD, CAT, GST,

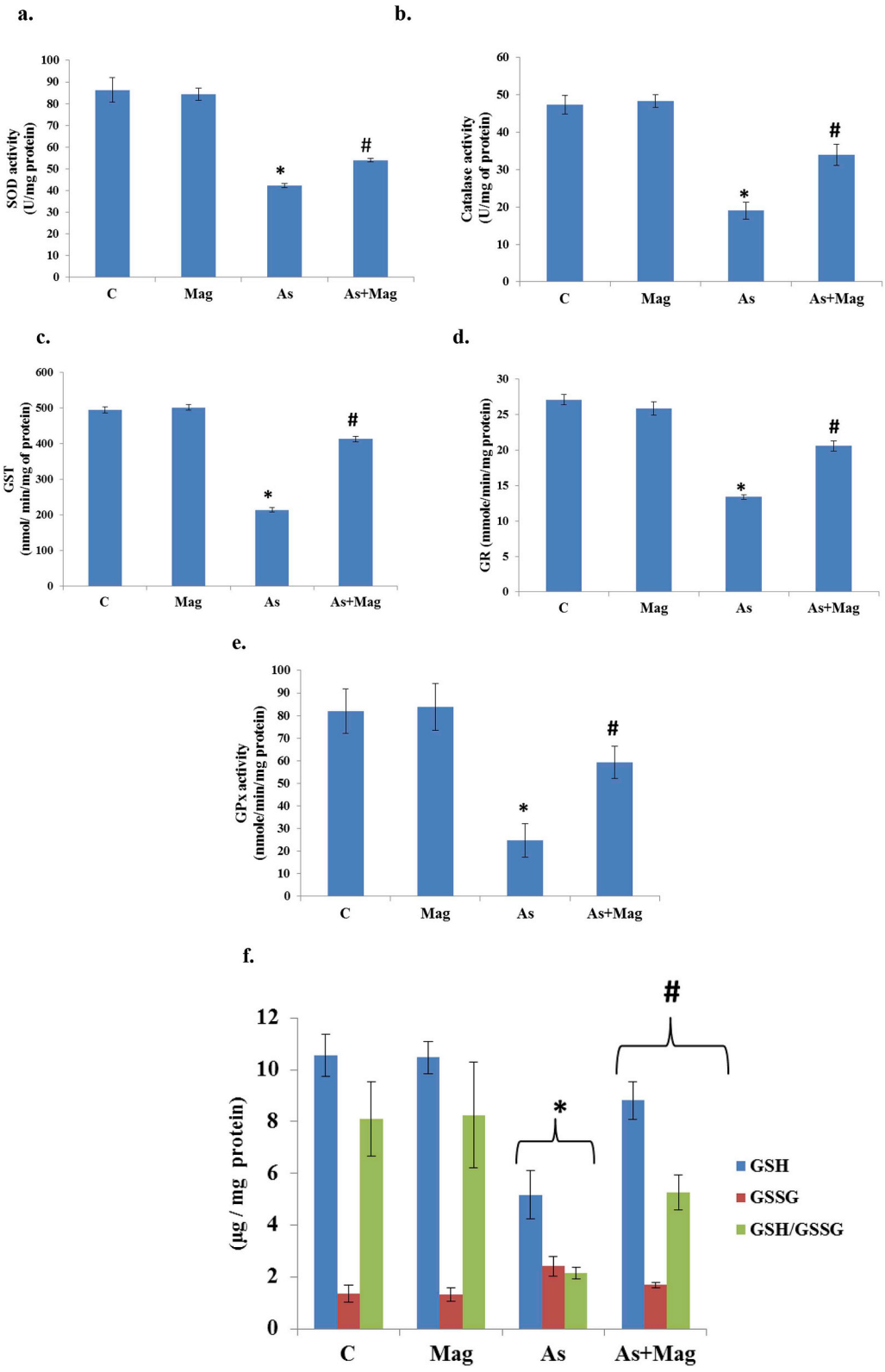

Fig. 9. Effect of arsenic (As) and mangiferin (Mag) on oxidative stress associated parameters:**(a,b,c,d,e)** Activity of various antioxidant enzymes (SOD, CAT, GST, GR, GPx), **(f)** cellular glutathione level (GSH, GSSG, and their ratio) in the lung tissue of the experimental mice. C: normal control mice; Mag: mangiferin administered mice; As: arsenic intoxicated mice; As + Mag: mangiferin post treated arsenic intoxicated mice. Each data represents the mean ± SD of 5 independent experiments for each individual group. *Significant difference between the control and As-exposed toxic group (*$P < 0.05$). #Significant difference between the arsenic exposed group and mangiferin post treated arsenic intoxicated group (#$P < 0.05$).

GR, and GPx which were reduced in As intoxicated lung. The principal non-enzymatic thiol-based antioxidant present in our body is glutathione. It sustains the redox regulation of cellular thiol proteins by post-translational modifications. Hence it exists in both reduced (GSH) and oxidized (GSSG) forms. In the normal homeostatic condition, the level of GSH is more than 90% whereas that of GSSG is less than 10%. When the body undergoes oxidative injury, GSH is oxidized into its disulfide form, GSSG, leading to altered homeostasis signifying stress induced pathophysiological conditions. Our investigation showed that in lung tissue of As exposed mice, the level of GSH was decreased whereas GSSG got elevated. These suppressed antioxidant defenses make the lung tissue more vulnerable to oxidative attack (Pisoschi and Pop, 2015). Further, this result correlated with the increased accumulation of As in the lung. Mangiferin, due to its C-glucosyl linkage and

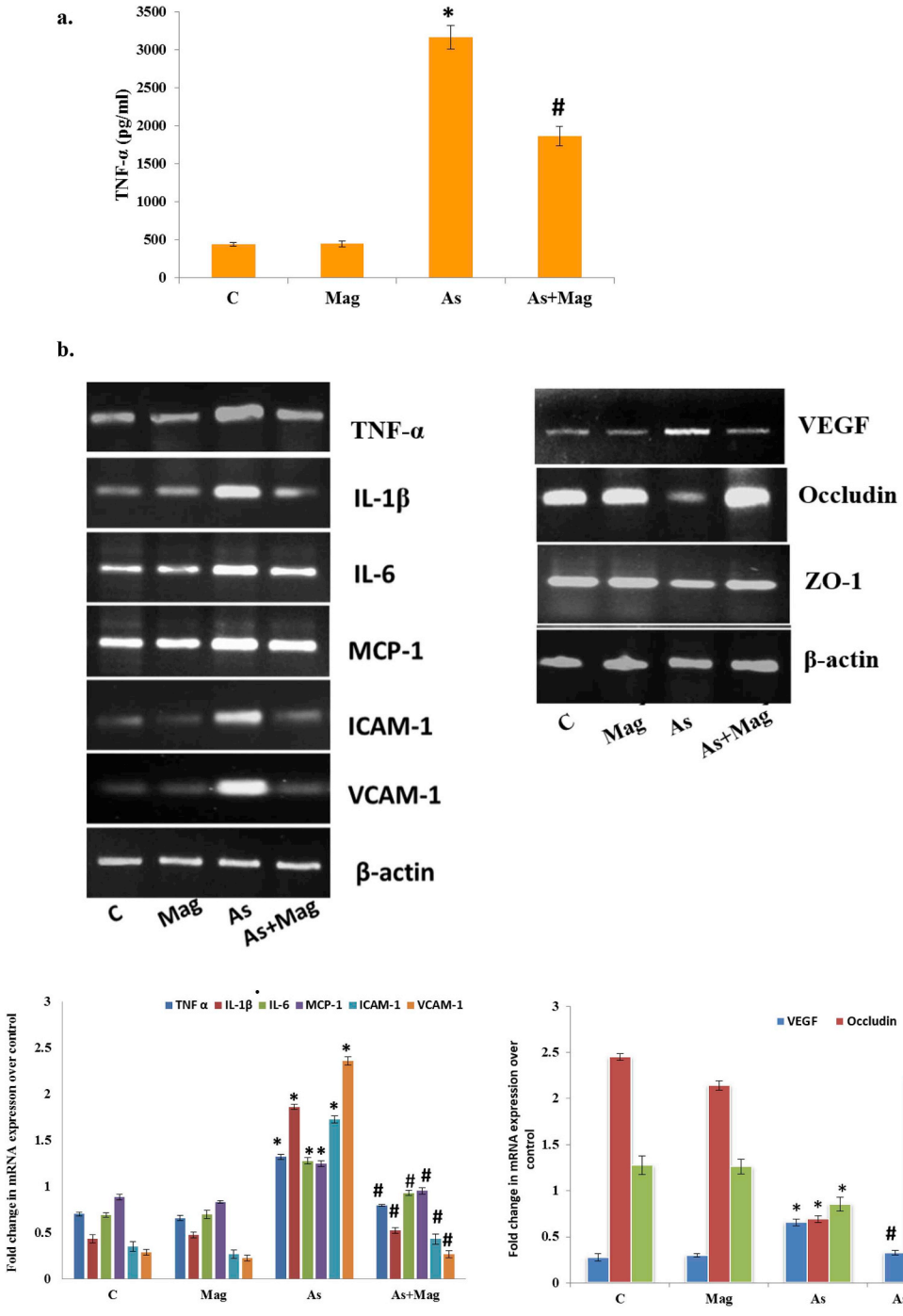

Fig. 10. (a) Level of TNF-α in BALF in the experimental animal groups. C: normal control mice; Mag: mangiferin administered mice; As: arsenic intoxicated mice; As + Mag: mangiferin post treatment after arsenic intoxicated mice; Each data represent the mean ± SD of 5 independent experiments for each individual group. *Significant difference between the control and arsenic exposed toxic group (*$P < 0.05$). #Significant difference between the arsenic exposed group and mangiferin post treated arsenic intoxicated group (#$P < 0.05$). **(b)** Quantitative RT-PCR gel images of TNF-α, IL-1β, IL−6, MCP-1, ICAM-1, VCAM-1, VEGF, Occludin, ZO-1. For internal control, β-actin was used. C: normal control mice; Mag: mangiferin administered mice; As: arsenic intoxicated mice; As + Mag: mangiferin post treatment after arsenic intoxicated mice; Densitometric data analysis represent mean ± SD for three different experimental group. "*"indicates significant difference between the control and arsenic exposed toxic group (*$P < 0.05$). "#"indicates significant difference between the arsenic exposed group and mangiferin-post treated group (#$P < 0.05$).

multiple −OH groups, neutralized the generated free radicals and consequently reduced LPO as well as protein carbonylation.

Besides crippling antioxidant status in biological system, ROS can also negatively modulate the protein activity at post-translational level and alter gene expression by regulating significant transcriptional factors, which along with MPO, promote an additional inflammatory environment (Manna et al., 2005; Ravichandran et al., 2010, 2011). TNF-α, a pro-inflammatory pleiotropic cytokine, is produced from monocytes and alveolar macrophages and causes severe lung injury by initiating inflammatory cascade. BALF of As intoxicated mice showed elevated level of TNF-α. Study revealed that TNF-α might exhibit paracrine mode of signaling on neutrophil requirement instead of endocrine effect (Lo et al., 1992; Pittet et al., 1997). Thus increased tissue level of TNF-α at mRNA and protein levels were correlated with neutrophil requirements in As exposed lung. This increased TNF-α subsequently led to the activation of various cytokines like IL-1β and IL-6 that caused endothelium activation and stimulated endothelial expression of adhesion molecules like MCP-1, ICAM-1, and VCAM-1. It also promoted leukocyte chemotaxis, resulting in a local inflammatory response in the lung. TNF-α and IL-1β also induced VEGF synthesis in As intoxicated lung. VEGF is normally expressed in lung (Brown et al., 1993), and upregulated VEGF expression is associated with increased capillary permeability (Senger et al., 1983).

TNF-α also reduced the expression of tight junctional protein like Occludin, (a transmembrane protein) and ZO-1 (a cytoplasmic protein) both of which play an important role to construct alveolar–capillary barrier (to maintain normal pulmonary function). When we performed Evans blue assay, enhanced dye uptake by As intoxicated lung was

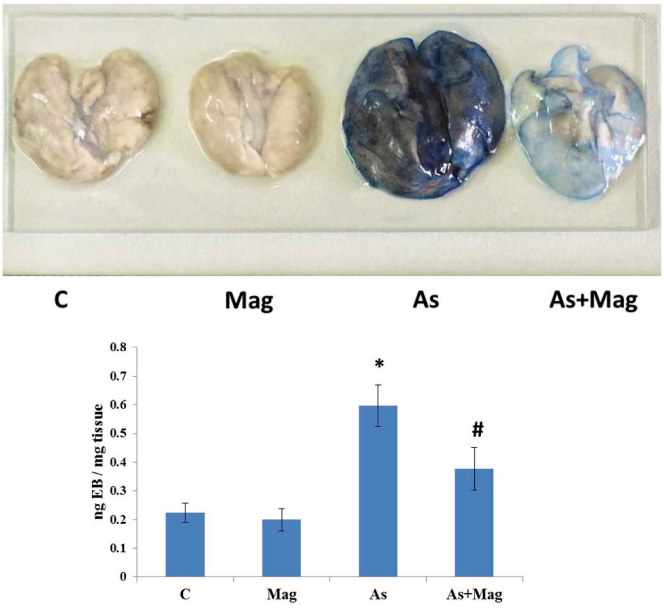

Fig. 11. The disruption of alveolar-capillary barrier by Evans blue extravasation (μg/g tissue) in Swiss albino mice. C: normal control mice; Mag: mangiferin administered mice; As: arsenic intoxicated mice; As + Mag: mangiferin post treatment after arsenic intoxication; Each data represents the mean ± SD of 5 independent experiments for each individual group. *Significant difference between the control and arsenic exposed toxic group (*$P < 0.05$). #Significant difference between the arsenic exposed group and mangiferin post treated arsenic intoxicated group (#$P < 0.05$). (For interpretation of the references to color in this figure legend, the reader is referred to the Web version of this article.)

correlated with the scenario that As breached endothelial barrier permeability by upregulating VEGF, and downregulating Occludin and ZO-1. Increased vascular permeability allowed extravasation of water in lung tissue. In normal condition, the excess water is pumped out of the lung with the help of Na^+/K^+-ATPase. So, we investigated whether increased lung W/D ratio was due to Na^+/K^+-ATPase dysfunction. Basolaterally located Na^+/K^+-ATPase in alveolar epithelial cells (AEC)

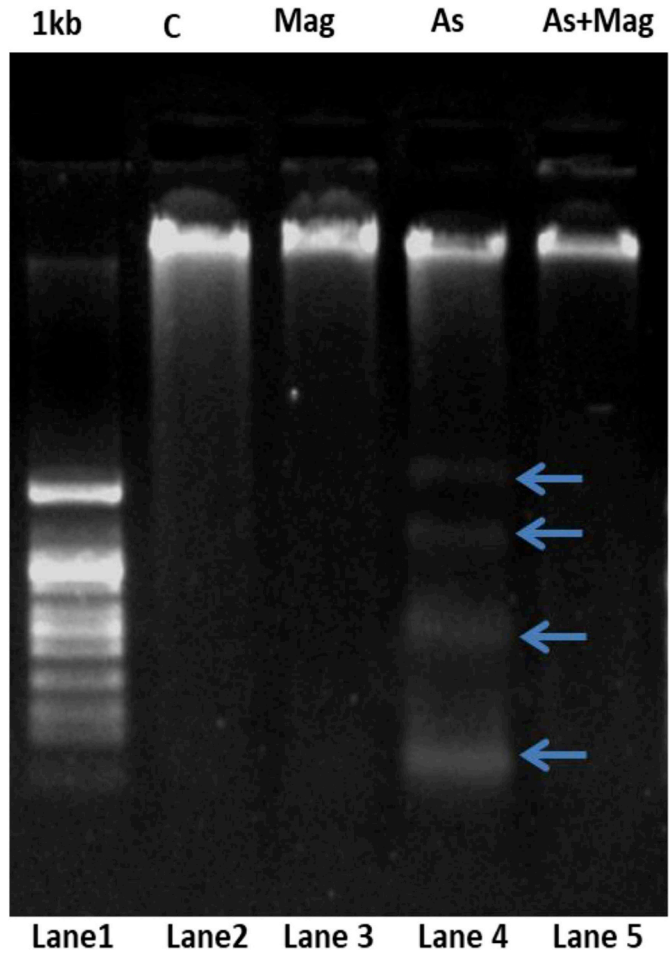

Fig. 13. Detection of arsenic-induced apoptosis in experimental mice by DNA fragmentation assay. Lane 1: Marker (1 kb DNA ladder); Lane 2: Isolated genomic DNA from normal control lung tissue; Lane 3: Isolated genomic DNA from mangiferin treated lung tissue; Lane 4: Isolated genomic DNA from arsenic intoxicated lung tissue; Lane 5: Isolated genomic DNA from lung tissue of mangiferin post treated arsenic intoxicated lung tissue.

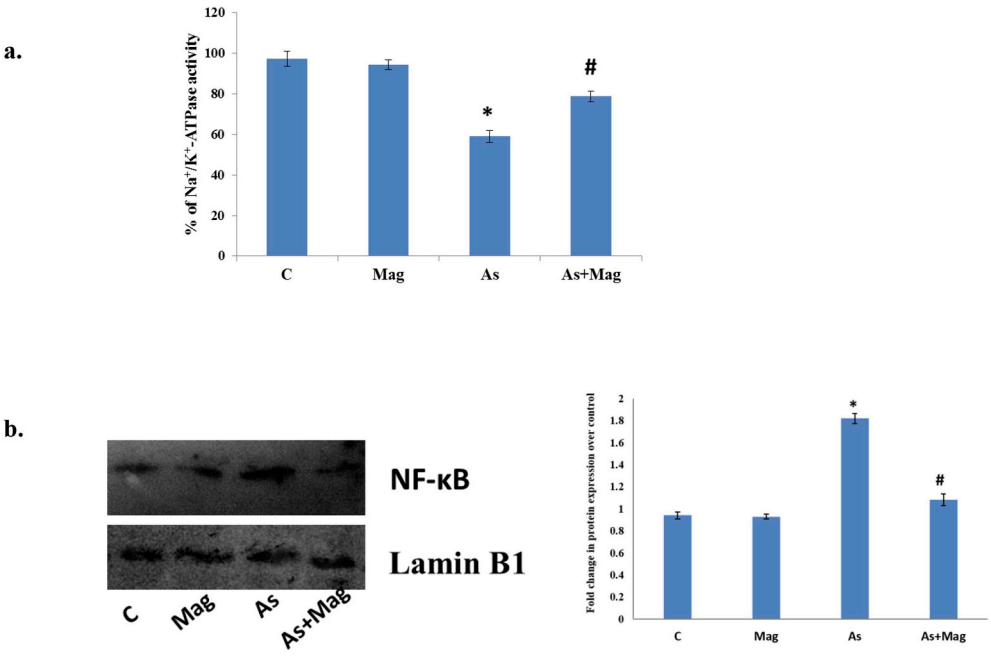

Fig. 12. (a) Na^+/K^+-ATPase activity in different groups of experimental mice. C: normal control mice; Mag: mangiferin administered mice; As: arsenic-intoxicated mice; As + Mag: mangiferin post treatment after arsenic intoxication; Each Data represent mean ± SD of 5 independent experiments for each individual group. *Significant difference between the control and arsenic exposed toxic group (*$P < 0.05$). #Significant difference between the arsenic exposed group and mangiferin post treated arsenic intoxicated group (#$P < 0.05$). **(b)** Immunoblot analysis of NF-κB. For internal control, LaminB1 was used. C: normal control mice; Mag: mangiferin administered mice; As: arsenic-intoxicated mice; As + Mag: mangiferin post treatment after arsenic intoxication; Densitometric data analysis represent mean ± SD for three different experimental group. "*"indicates significant difference between the control and arsenic exposed toxic group (*$P < 0.05$). "#"indicates significant difference between the arsenic exposed group and mangiferin-post treated group (#$P < 0.05$).

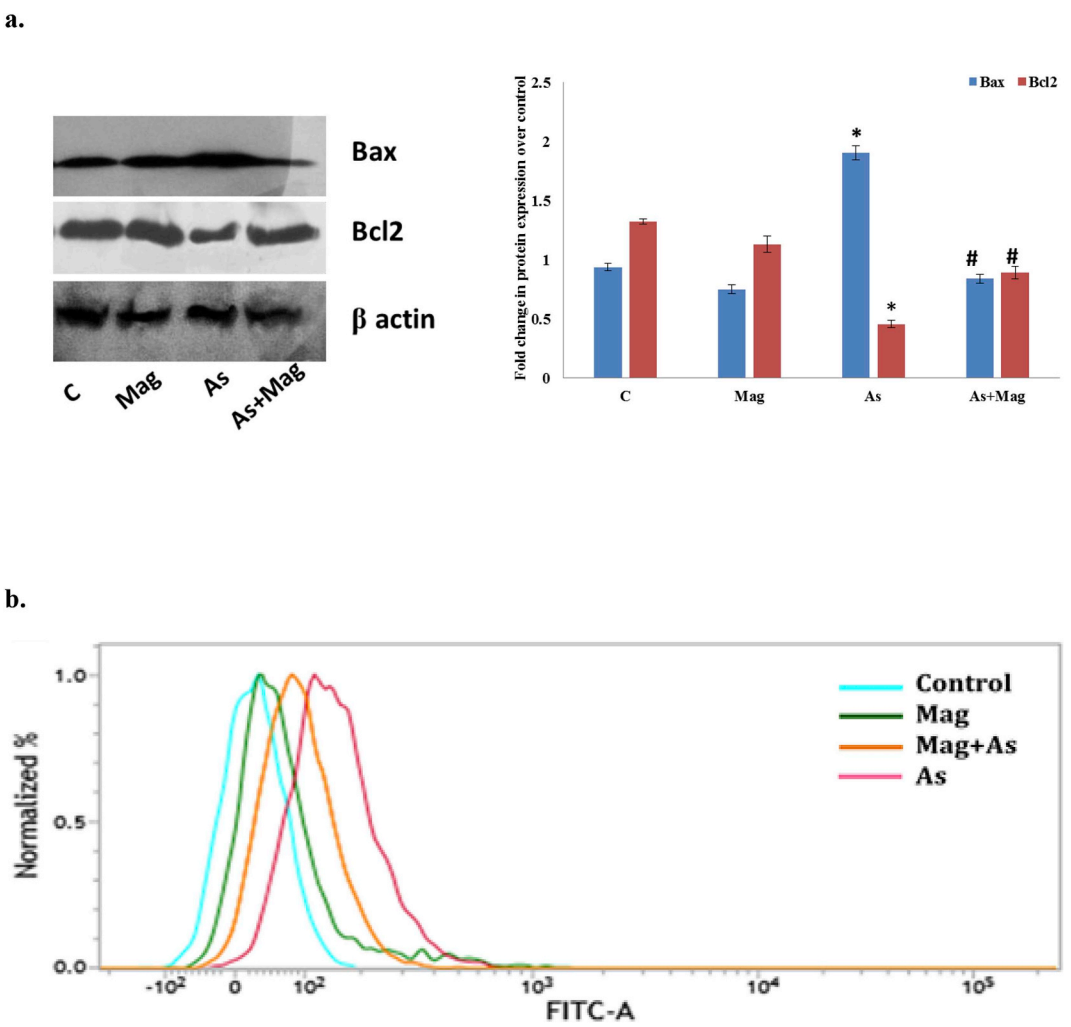

Fig. 14. (a) Immunoblot analysis showing expression of Bax and Bcl2. For internal control, β-actin was used. C: normal control mice; Mag: mangiferin administered mice; As: arsenic intoxicated mice; As + Mag: mangiferin post treated arsenic intoxicated mice. Densitometric data analysis represent mean ± SD for three different experimental group. "*"indicates significant difference between the control and arsenic exposed toxic group ($*P < 0.05$). "#"indicates significant difference between the arsenic exposed group and mangiferin-post treated group ($\#P < 0.05$). **(b)** Flow cytometric analysis of mitochondrial membrane potential (MMP) of lung tissue in different experimental mice groups. MMP was measured by the fluorescence intensity of JC1. JC1 showed a decrease in MMP upon arsenic intoxication. Mangiferin post treatment increased MMP in the experimental animals. C: normal control mice; Mag: mangiferin administered mice; As: arsenic intoxicated mice; As + Mag: mangiferin post treated arsenic intoxicated mice.

pumps Na^+ across the basal membrane. The resulting ionic gradient causes passive movement of water through channels in AEC and thus regulated alveolar fluid clearance (Sartori et al., 2010). The current study explored that As inhibited Na^+/K^+- ATPase function which was due to increased LPO. Moreover, NF-κB negatively regulates Na^+/K^+-ATPase activity by decreasing copy number of subunit α1 - Na^+/K^+-ATPase (Mathew and Sarada, 2015). Here in our study, TNF-α further upregulated the transcription factor NF-κB, which in turn downregulated Na^+/K^+-ATPase activity. Insufficiency of this transport protein activity hampered the alveolar fluid clearance and increased wet weight of lung. Mangiferin, being a powerful anti-inflammatory molecule, successfully downregulated the levels of TNF-α and NF-κB, thus restoring the Na^+/K^+-ATPase activity in AEC to maintain the flow of alveolar fluid clearance.

As induced oxidative damage perturb the normal cellular homeostasis by inducing cell death. Therefore, we checked the mode of cell death and observed the appearance of fragmented genomic DNA in As intoxicated group (confirming apoptotic mode of cell death). As TNF-α is responsible for extra mitochondrial mode of apoptotic pathway (Sedger and McDermott, 2014) and its level was highly elevated in BALF and lung of As administered group, expression of its downstream signaling molecule caspase 8 was quantified. Increased expression of caspase 8 ensured TNF-α induced lung cell apoptosis. Moreover, we also found decreased MMP due to altered Bax/Bcl2 ratio causing the release of cytochrome c from mitochondria to cytosol in intoxicated lung. This cytosolic cytochrome c led to the activation of caspase 9 and 3, triggering apoptosis. Mangiferin remarkably downregulated these apoptotic molecules, confirming its effectiveness against As intoxication.

Evidence suggests that TNF-α can initiate ER stress and prolonged ER stress is also responsible for apoptotic mode of cell death (Oyadomari and Mori, 2004; Ghosh et al., 2010). In As intoxicated lung tissue, we found elevated expression of JNK which in turn triggered ER stress related downstream molecules CHOP and caspase 12. Moreover, increased PKCδ, due to the synchronous effect of ER stress and elevated NF-κB expression, further caused JNK activation. Immunofluorescence study also revealed the increased expression of TNF-α and its downregulation by mangiferin in As intoxicated lung.

Next, we attempted to investigate the possible signaling mechanisms which are activated by mangiferin to exert pulmonary protective effects. An upregulated expression of Nrf2 protein in As intoxicated mice was detected by western blotting after mangiferin administration.

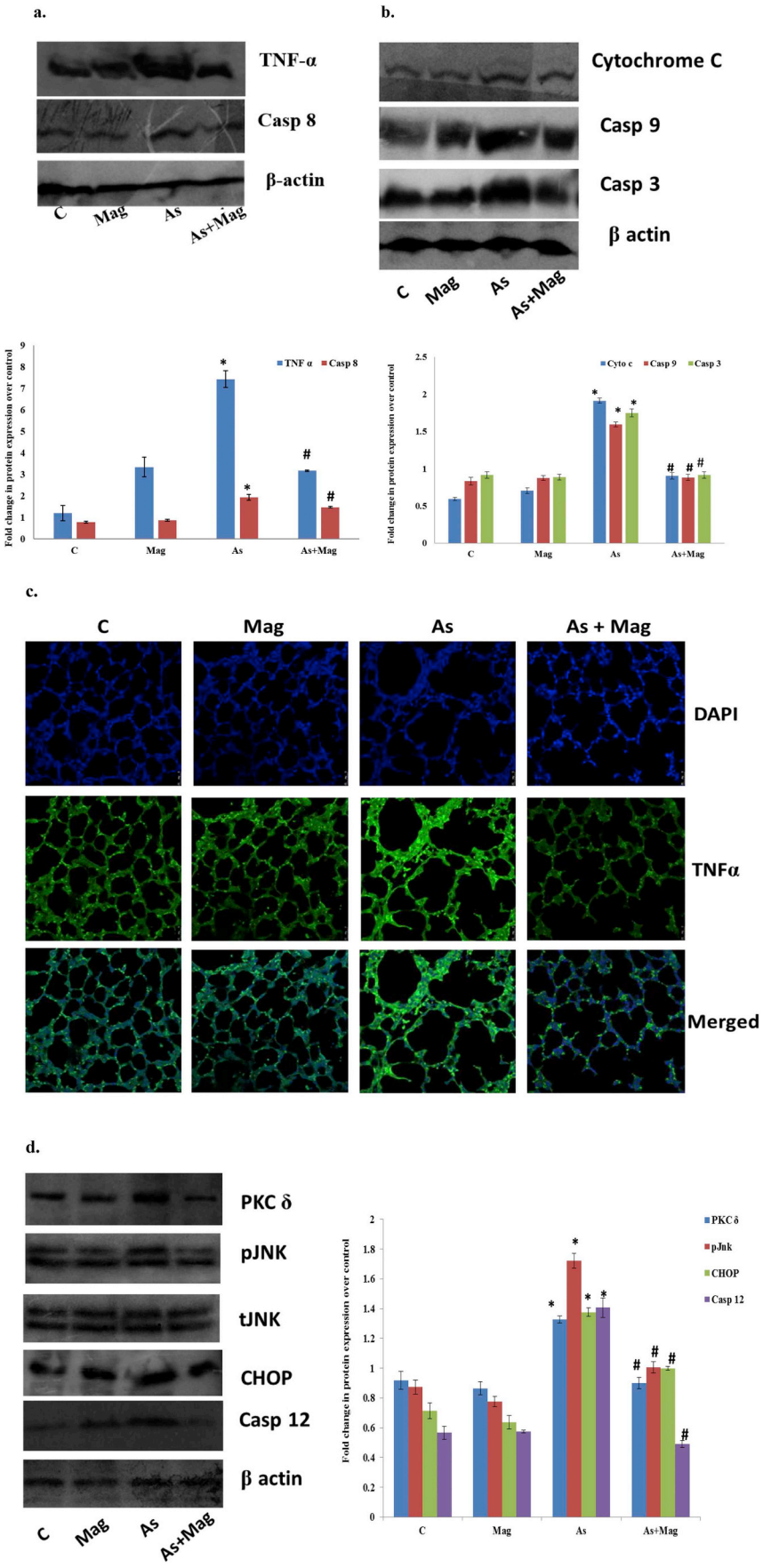

Fig. 15. Immunoblot analysis showing expression of various signaling molecule related to apoptotic pathway in response to arsenic. **(a)** Analysis of extrinsic death pathway molecules TNF-α, Caspase 8 by western blot. **(b)** Immunoblot analysis of intrinsic pathway of apoptotic molecules Cytochrome C, Caspase 9, Caspase 3. **(c)** Immunofluorescence micrographs of lung tissue section showing the expression of TNF-α. **(d)** Immunoblot analysis of molecules related to ER stress mainly PKC δ, JNK, CHOP, and Caspase 12. For internal control, β-actin was used. C: normal control mice; Mag: mangiferin administered mice; As: arsenic intoxicated mice; As + Mag: mangiferin post treatment post treated arsenic intoxicated mice. Densitometric data analysis represent mean ± SD for three different experimental groups. "*"indicates significant difference between the control and arsenic exposed toxic group ($*P < 0.05$). "#"indicates significant difference between the arsenic exposed group and mangiferin-post treated group ($\#P < 0.05$).

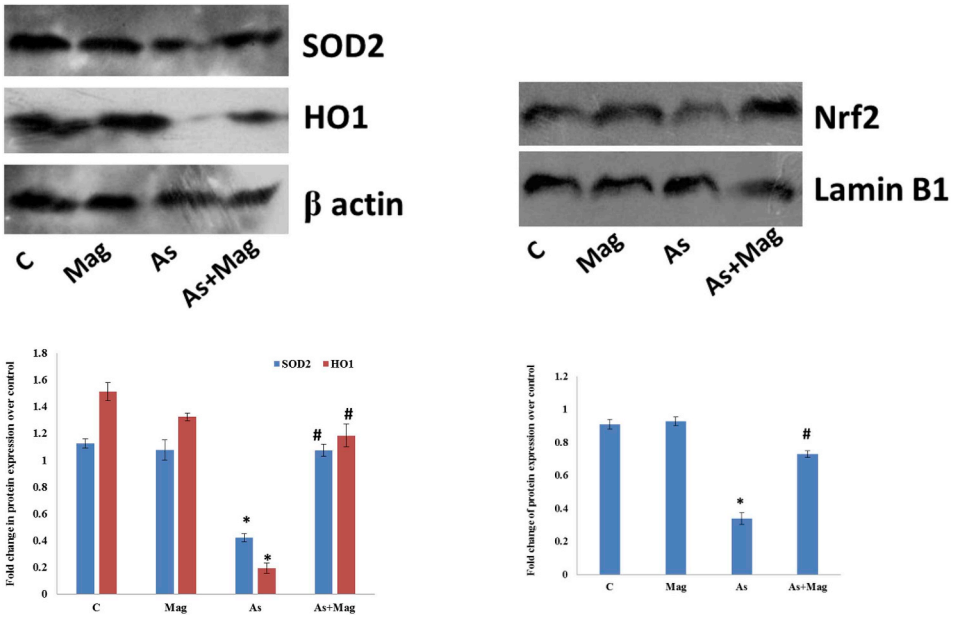

Fig. 16. Immunoblot analysis of molecules Nrf2 and its downstream HO1, SOD2. For internal control, β-actin and Lamin B1 were used. C: normal control mice; Mag: mangiferin administered mice; As: arsenic intoxicated mice; As + Mag: mangiferin post treated arsenic intoxicated mice. Densitometric data analysis represent mean ± SD for three different experimental groups. "*"indicates significant difference between the control and arsenic exposed toxic group ($*P < 0.05$). "#"indicates significant difference between the arsenic exposed group and mangiferin-post treated group ($\#P < 0.05$).

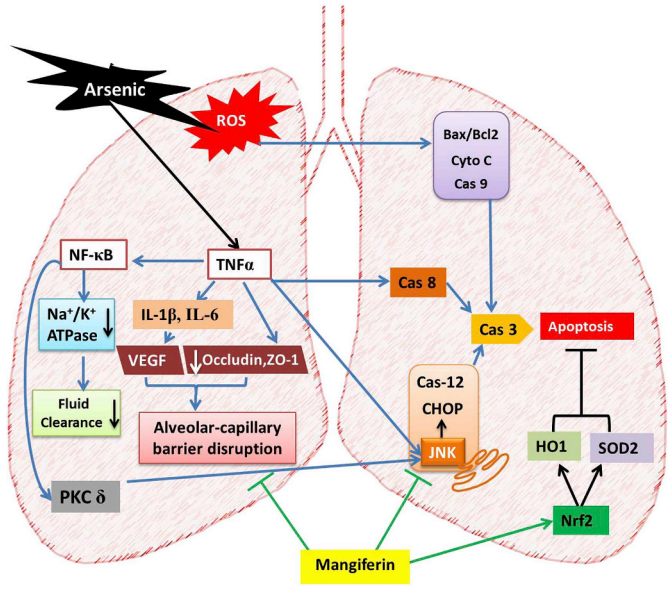

Fig. 17. Schematic illustration showing different signaling molecules involved in arsenic and mangiferin exposure. As induced oxidative stress and led to the activation of both intrinsic and extrinsic apoptotic molecules resulting in caspase 3 induced apoptosis. Additionally, it also led to JNK mediated ER stress along with mitochondrial depolarization. Further, As also activated pro-inflammatory molecules like TNF-α and NF-κB, causing alveolar capillary barrier disruption and damaged the lung. Mangiferin, on other hand, downregulated all pro-inflammatory and pro-apoptotic molecules. It also activated Nrf2 and caused upregulation of endogenous anti-oxidants thus showing amelioration against As induced pulmonary toxicity.

Nrf2 is considered to play a pivotal role to maintain the endogenous redox balance. It induced the synthesis of antioxidants SOD2 and HO1and thereby protected the As induced lung injury. The potential mechanisms involved in As induced toxicity and protection by mangiferin is represented in Fig. 17.

5. Conclusion

Our results suggested that mangiferin, a xanthonoid, ameliorated As induced lung injury by mitigating oxidative stress. Antioxidant and anti-inflammatory nature of mangiferin helped to restore cellular antioxidant status, prevented inflammatory outburst and inhibited apoptosis. Thus mangiferin can be considered as a promising natural molecule against such pulmonary complication.

Transparency document

Transparency document related to this article can be found online at https://doi.org/10.1016/j.fct.2019.02.022.

References

Andrew, A.S., Bernardo, V., Warnke, L.A., Davey, J.C., Hampton, T., Mason, R.A., Thorpe, J.E., Ihnat, M.A., Hamilton, J.W., 2007. Exposure to arsenic at levels found in U.S. drinking water modifies expression in the mouse lung. Toxicol. Sci. 100, 75–87.
Bhattacharya, S., 2017. Medicinal plants and natural products in amelioration of arsenic toxicity: a short review. Pharmaceut. Biol. 55 (1), 349–354.
Boellmann, F., Zhang, L., Clewell, H.J., Schroth, G.P., Kenyon, E.M., Andersen, M.E., Thomas, R.S., 2010. Genome-wide analysis of DNA methylation and gene expression changes in the mouse lung following subchronic arsenate exposure. Toxicol. Sci. 117, 404–417.
Brown, L.F., Berse, B., Jackman, R.W., Tognazzi, K., Manseau, E.J., Senger, D.R., Dvorak, H.F., 1993. Expression of vascular permeability factor (vascular endothelial growth factor) and its receptors in adenocarcinomas of the gastrointestinal tract. Cancer Res. 53, 4727–4735.
Bulka, C.M., Jones, R.M., Turyk, M.E., Stayner, L.T., Argos, M., 2016. Arsenic in drinking water and prostate cancer in Illinois counties: an ecologic study. Environ. Res. 148, 450–456.
Chakraborti, D., Rahman, M.M., Das, B., Murrill, M., Dey, S., Mukherjee, S.C., Dhar, R.K., Biswas, B.K., Chowdhury, U.K., Roy, S., 2010. Status of groundwater arsenic contamination in Bangladesh: a 14-year study report. Water Res. 44, 5789–5802.
Chowdhury, U.K., Biswas, B.K., Chowdhury, T.R., Samanta, G., Mandal, B.K., Basu, G.C., Chanda, C.R., Lodh, D., Saha, K.C., Mukherjee, S.K., Roy, S., Kabir, S., Quamruzzaman, Q., Chakraborti, D., 2000. Groundwater arsenic contamination in Bangladesh and West Bengal, India. Environ. Health Perspect. 108, 393–397.
Das, D., Bindhani, B., Mukherjee, B., Saha, H., Biswas, P., Dutta, K., Prasad, P., Sinha, D., Ray, M.R., 2014. Chronic low-level arsenic exposure reduces lung function in male population without skin lesions. Int. J. Public Health 59, 655–663.
Das, D., Samanta, G., Mandal, B.K., Chowdhury, T.R., Chanda, C.R., Chowdhury, P.P., Basu, G.K., Chakraborti, D., 1996. Arsenic in groundwater in six districts of West Bengal, India. Environ. Geochem. Health 18, 5–15.
Das, J., Ghosh, J., Roy, A., Sil, P.C., 2012a. Mangiferin exerts hepatoprotective activity against D-galactosamine induced acute toxicity and oxidative/nitrosative stress via Nrf2-NFkappaB pathways. Toxicol. Appl. Pharmacol. 260, 35–47.
Das, J., Roy, A., Sil, P.C., 2012b. Mechanism of the protective action of taurine in toxin and drug induced organ pathophysiology and diabetic complications: a review. Food and function 3, 1251–1264.
Das, J., Ghosh, J., Manna, P., Sinha, M., Sil, P.C., 2009. Arsenic-induced oxidative cerebral disorders: protection by taurine. Drug Chem. Toxicol. 32, 93–102.
Dauphine, D.C., Ferreccio, C., Guntur, S., Yuan, Y., Hammond, S.K., Balmes, J., Smith, A.H., Steinmaus, C., 2011. Lung function in adults following in utero and childhood

exposure to arsenic in drinking water: preliminary findings. Int. Arch. Occup. Environ. Health 84, 591–600.
Dutta, S., Saha, S., Mahalanobish, S., Sadhukhan, P., Sil, P.C., 2018. Melatonin attenuates arsenic induced nephropathy via the regulation of oxidative stress and inflammatory signaling cascades in mice. Food Chem. Toxicol. 118, 303–316.
García-Vargas, G.G., García-Rangel, A., Aguilar-Romo, M., García-Salcedo, J., del Razo, L.M., Ostrosky-Wegman, P., Cortinas de Nava, C., Cebrián, M.E., 1991. A pilot study on the urinary excretion of porphyrins in human populations chronically exposed to arsenic in Mexico. Hum. Exp. Toxicol. 10, 189–193.
Ghosh, J., Sil, P.C., 2013. Arjunolic acid: a new multifunctional therapeutic promise of alternative medicine. Biochime 95, 1098–1109.
Ghosh, J., Das, J., Manna, P., Sil, P.C., 2010. Hepatotoxicity of di-(2-ethylhexyl) phthalate is attributed to calcium aggravation, ROS-mediated mitochondrial depolarization, and ERK/NF-kappaB pathway activation. Free Radic. Biol. Med. 49, 1779–1791.
Ghosh, M., Das, J., Sil, P.C., 2012. D (+) galactosamine induced oxidative and nitrosative stress-mediated renal damage in rats via NF-κB and inducible nitric oxide synthase (iNOS) pathways is ameliorated by a polyphenol xanthone, mangiferin. Free Radic. Res. 46, 116–132.
Guha, S., Ghosal, S., Chattopadhyay, U., 1996. Antitumor, immunomodulatory and anti-HIV effect of mangiferin, a naturally occurring glucosylxanthone. Chemotherapy 42, 443–451.
Harris, Z., Ridge, K., Gonzalez-Flecha, B., Gottlieb, L., Zucker, A., Sznajder, J., 1996. Hyperbaric oxygenation upregulates rat lung Na, K-ATPase. Eur. Respir. J. 9, 472–477.
Hashizume, M., Mouner, M., Chouteau, J.M., Gorodnya, O.M., Ruchko, M.V., Wilson, G.L., Gillespie, M.N., Parker, J.C., 2014. Mitochondrial targeted endonuclease III DNA repair enzyme protects against ventilator induced lung injury in mice. Pharmaceuticals 7, 894–912.
Healy, S.M., Casarez, E.A., Ayala-Fierro, F., Aposhian, H., 1998. Enzymatic methylation of arsenic compounds. V. Arsenite methyltransferase activity in tissues of mice. Toxicol. Appl. Pharmacol. 148, 65–70.
Henderson, M.W., Madenspacher, J.H., Whitehead, G.S., Thomas, S.Y., Aloor, J.J., Gowdy, K.M., Fessler, M.B., 2017. Effects of orally ingested arsenic on respiratory epithelial permeability to bacteria and small molecules in mice. Environ. Health Perspect. 125.
Hissin, P.J., Hilf, R., 1976. A fluorometric method for determination of oxidized and reduced glutathione in tissues. Anal. Biochem. 74, 214–226.
Huang, Q., Bu, S., Yu, Y., Guo, Z., Ghatnekar, G., Bu, M., Yang, L., Lu, B., Feng, Z., Liu, S., Wang, F., 2007. Diazoxide prevents diabetes through inhibiting pancreatic beta-cells from apoptosis via Bcl-2/Bax rate and p38-beta mitogen-activated protein kinase. Endocrinology 148, 81–91.
Hughes, M.F., Beck, B.D., Chen, Y., Lewis, A.S., Thomas, D.J., 2011. Arsenic exposure and toxicology: a historical perspective. Toxicol. Sci. 123, 305–332.
Hughes, M.F., Kenyon, E.M., Edwards, B.C., Mitchell, C.T., Razo, L.M., Thomas, D.J., 2003. Accumulation and metabolism of arsenic in mice after repeated oral administration of arsenate. Toxicol. Appl. Pharmacol. 191, 202–210.
Kenyon, E.M., Del Razo, L.M., Hughes, M.F., 2005. Tissue distribution and urinary excretion of inorganic arsenic and its methylated metabolites in mice following acute oral administration of arsenate. Toxicol. Sci. 85, 468–475.
Kim, Y.J., Kim, J.M., 2015. Arsenic toxicity in male reproduction and development. Development & Reproduction 19, 167–180.
Lampl, T., Crum, J.A., Davis, T.A., Milligan, C., Del Gaizo Moore, V., 2015. Isolation and functional analysis of mitochondria from cultured cells and mouse tissue. JoVE : JoVE 97, 52076.
Leonard, S.S., Harris, G.K., Shi, X., 2004. Metal-induced oxidative stress and signal transduction. Free Radic. Biol. Med. 37, 1921–1942.
Lo, S.K., Everitt, J., Gu, J., Malik, A.B., 1992. Tumor necrosis factor mediates experimental pulmonary edema by ICAM-1 and CD18-dependent mechanisms. J. Clin. Invest. 89, 981–988.
Lynch, H.N., Zu, K., Kennedy, E.M., Lam, T., Liu, X., Pizzurro, D.M., Loftus, C.T., Rhomberg, L.R., 2017. Quantitative assessment of lung and bladder cancer risk and oral exposure to inorganic arsenic: meta-regression analyses of epidemiological data. Environ. Int. 106, 178–206.
Manna, P., Sinha, M., Pal, P., Sil, P.C., 2007. Arjunolic acid, a triterpenoid saponin, ameliorates arsenic-induced cyto-toxicity in hepatocytes. Chem. Biol. Interact. 170, 187–200.
Manna, S.K., Sarkar, S., Barr, J., Wise, K., Barrera, E.V., Jejelowo, O., Rice-Ficht, A.C., Ramesh, G.T., 2005. Single-walled carbon nanotube induces oxidative stress and activates nuclear transcription factor-κB in human keratinocytes. Nano Lett. 5, 1676–1684.
Mathew, T., Sarada, S., 2015. Attenuation of NFkB activation augments alveolar transport proteins expression and activity under hypoxia. Int. J. Sci. Res. 4, 2230–2237.
Matsuyama, H., Amaya, F., Hashimoto, S., Ueno, H., Beppu, S., Mizuta, M., Shime, N., Ishizaka, A., Hashimoto, S., 2008. Acute lung inflammation and ventilator-induced lung injury caused by ATP via the P2Y receptors: an experimental study. Respir. Res. 9, 79.
Mazumder, D.N.G., Haque, R., Ghosh, N., De, B.K., Santra, A., Chakraborty, D., Smith, A.H., 1998. Arsenic levels in drinking water and the prevalence of skin lesions in West Bengal, India. Int. J. Epidemiol. 27, 871–877.
Moreira, R.R., Carlos, I.Z., Vilega, W., 2001. Release of intermediate reactive hydrogen peroxide by macrophage cells activated by natural products. Biol. Pharm. Bull. 24, 201–204.
Oyadomari, S., Mori, M., 2004. Roles of CHOP/GADD153 in endoplasmic reticulum stress. Cell Death Differ. 11, 381.
Pal, P.B., Sinha, K., Sil, P.C., 2014. Mangiferin attenuates diabetic nephropathy by inhibiting oxidative stress mediated signaling cascade, TNFalpha related and mitochondrial dependent apoptotic pathways in streptozotocin-induced diabetic rats. PLoS One 9, e107220.
Pal, P.B., Sinha, K., Sil, P.C., 2013. Mangiferin, a natural xanthone, protects murine liver in Pb(II) induced hepatic damage and cell death via MAP kinase, NF-kappaB and mitochondria dependent pathways. PLoS One 8, e56894.
Parvez, F., Chen, Y., Brandt-Rauf, P.W., Bernard, A., Dumont, X., Slavkovich, V., Argos, M., D'Armiento, J., Foronjy, R., Hasan, M.R., Eunus, H.E., Graziano, J.H., Ahsan, H., 2008. Nonmalignant respiratory effects of chronic arsenic exposure from drinking water among never-smokers in Bangladesh. Environ. Health Perspect. 116, 190–195.
Perelman, A., Wachtel, C., Cohen, M., Haupt, S., Shapiro, H., Tzur, A., 2012. JC-1: alternative excitation wavelengths facilitate mitochondrial membrane potential cytometry. Cell Death & Disease 3, e430.
Pisoschi, A.M., Pop, A., 2015. The role of antioxidants in the chemistry of oxidative stress: a review. Eur. J. Med. Chem. 97, 55–74.
Pittet, J., Mackersie, R., Martin, T., Matthay, M., 1997. Biological markers of acute lung injury: prognostic and pathogenetic significance. Am. J. Respir. Crit. Care Med. 155, 1187–1205.
Rashid, K., Sil, P., 2015. Curcumin enhances recovery of pancreatic islets from cellular stress induced inflammation and apoptosis in diabetic rats. Toxicol. Appl. Pharmacol. 282, 297–310.
Rashid, K., Sinha, K., Sil, P.C., 2013. An update on oxidative stress-mediated organ pathophysiology. Food Chem. Toxicol.: Inter. J. Publ. Brit. Ind. Biol. Res. Assoc. 62, 584–600.
Ravichandran, P., Baluchamy, S., Gopikrishnan, R., Biradar, S., Ramesh, V., Goornavar, V., Thomas, R., Wilson, B.L., Jeffers, R., Hall, J.C., 2011. Pulmonary biocompatibility assessment of inhaled single-wall and multiwall carbon nanotubes in BALB/c mice. J. Biol. Chem. 286, 29725–29733.
Ravichandran, P., Baluchamy, S., Sadanandan, B., Gopikrishnan, R., Biradar, S., Ramesh, V., Hall, J.C., Ramesh, G.T., 2010. Multiwalled carbon nanotubes activate NF-κB and AP-1 signaling pathways to induce apoptosis in rat lung epithelial cells. Apoptosis 15, 1507–1516.
Recio-Vega, R., Gonzalez-Cortes, T., Olivas-Calderon, E., Lantz, R.C., Gandolfi, A.J., Gonzalez-De Alba, C., 2015. In utero and early childhood exposure to arsenic decreases lung function in children. J. Appl. Toxicol. : JAT 35, 358–366.
Rodeiro, I., Delgado, R., Garrido, G., 2014. Effects of a Mangifera indica L. stem bark extract and mangiferin on radiation-induced DNA damage in human lymphocytes and lymphoblastoid cells. Cell Prolif 47, 48–55.
Saha, S., Sadhukhan, P., Mahalanobish, S., Dutta, S., Sil, P.C., 2018. Ameliorative role of genistein against age-dependent chronic arsenic toxicity in murine brains via the regulation of oxidative stress and inflammatory signaling cascades. J. Nutr. Biochem. 55, 26–40.
Saha, S., Sadhukhan, P., Sil, P.C., 2016. Mangiferin: a xanthonoid with multipotent anti-inflammatory potential. Biofactors 42, 459–474.
Saleh, S., El-Maraghy, N., Reda, E., Barakat, W., 2014. Modulation of diabetes and dyslipidemia in diabetic insulin-resistant rats by mangiferin: role of adiponectin and TNF-α. An. Acad. Bras. Cienc. 86, 1935–1948.
Sarkar, K., Sil, P.C., 2006. A 43 kDa protein from the herb Cajanus indicus L. protects thioacetamide induced cytotoxicity in hepatocytes. Toxicol. Vitro 20, 634–640.
Sartori, C., Rimoldi, S.F., Scherrer, U., 2010. Lung fluid movements in hypoxia. Prog. Cardiovasc. Dis. 52, 493–499.
Sedger, L.M., McDermott, M.F., 2014. TNF and TNF-receptors: from mediators of cell death and inflammation to therapeutic giants–past, present and future. Cytokine & growth factor reviews 25, 453–472.
Senger, D.R., Galli, S.J., Dvorak, A.M., Perruzzi, C.A., Harvey, V.S., Dvorak, H.F., 1983. Tumor cells secrete a vascular permeability factor that promotes accumulation of ascites fluid. Science 219, 983–985.
Sinha, K., Pal, P.B., Sil, P.C., 2013. Mangiferin, a naturally occurring xanthone C-glycoside, ameliorates lead (Pb)-induced murine cardiac injury via mitochondria-dependent apoptotic pathways. Signpost Open Access J Org Biomol Chem 1, 47–63.
Sinha, M., Manna, P., Sil, P.C., 2008. Protective effect of arjunolic acid against arsenic-induced oxidative stress in mouse brain. J. Biochem. Mol. Toxicol. 22, 15–26.
Sinha, M., Manna, P., Sil, P.C., 2007. Aqueous extract of the bark of Terminalia arjuna plays a protective role against sodium-fluoride-induced hepatic and renal oxidative stress. J. Nat. Med. 61, 251–260.
States, J.C., Srivastava, S., Chen, Y., Barchowsky, A., 2009. Arsenic and cardiovascular disease. Toxicol. Sci. 107, 312–323.
Tseng, C.H., 2009. A review on environmental factors regulating arsenic methylation in humans. Toxicol. Appl. Pharmacol. 235, 338–350.
Tyler, C.R., Allan, A.M., 2014. The effects of arsenic exposure on neurological and cognitive dysfunction in human and rodent studies: a review. Current Environmental Health Reports 1, 132–147.
Uchida, K., Stadtman, E., 1992. Selective cleavage of thioether linkage in proteins

modified with 4-hydroxynonenal. Proc. Natl. Acad. Sci. Unit. States Am. 89, 5611–5615.
von Ehrenstein, O.S., Mazumder, D.N., Yuan, Y., Samanta, S., Balmes, J., Sil, A., Ghosh, N., Hira-Smith, M., Haque, R., Purushothamam, R., Lahiri, S., Das, S., Smith, A.H., 2005. Decrements in lung function related to arsenic in drinking water in West Bengal, India. Am. J. Epidemiol. 162, 533–541.
Wei, M., Guo, F., Rui, D., Wang, H., Feng, G., Li, S., Song, G., 2018. Alleviation of arsenic-induced pulmonary oxidative damage by GSPE as shown during in vivo and in vitro experiments. Biol. Trace Elem. Res. 183, 80–91.
Yamanaka, K., Hasegawa, A., Sawamura, R., Okada, S., 1989. Dimethylated arsenics induce DNA strand breaks in lung via the production of active oxygen in mice. Biochem. Biophys. Res. Commun. 165, 43–50.
Yen, C.-C., Lu, F.-J., Huang, C.-F., Chen, W.-K., Liu, S.-H., Lin-Shiau, S.-Y., 2007. The diabetogenic effects of the combination of humic acid and arsenic: in vitro and in vivo studies. Toxicol. Lett. 172, 91–105.
Yoshimi, N., Matsunaga, K., Katayama, M., Yamada, Y., Kuno, T., Qiao, Z., Hara, A., Yamahara, J., Mori, H., 2001. The inhibitory effects of mangiferin, a naturally occurring glucosylxanthone, in bowel carcinogenesis of male F344 rats. Cancer Lett. 163, 163–170.